ISSN: 1999-6691, e-ISSN: 2782-3709 DOI: http://doi.org/10.7242/1999-6691/2024.17.1.11

Research article

Simulation of spherical layered system compression by shock waves with allowance for radiative heat transfer in different approximation

S.A. Grabovenskaya, V.V. Zaviyalov, A.A. Shestakov

FSUE "RFNC-VNIITF named after Akadem. E.I. Zababakhin", Snezhinsk, Russian Federation

Numerical modeling is one of the basic tools to investigate physical phenomena that occur in materials compressed by shock waves. A study of the behavior of shock waves using simplified models is helpful in the analysis of more complex systems, for instance, in the problems of inertial thermonuclear fusion on laser facilities. Mathematical simulation of the nonstationary radiative heat transfer in a spectral kinetic statement is rather complicated because the system of equations is nonlinear and large in size. Generally, the kinetic transport equation is solved in 7D phase space, which requires huge computational resources. The initial system is often approximated under certain assumptions but this immediately causes questions as to whether the simplified model is applicable to particular calculations. In this study, several economic radiative heat transfer models were implemented in a 2D hydrodynamic code. Based on these models, test calculations were performed to simulate the compression of a layered spherical system by shock waves, taking into account radiative heat transfer. When the shock wave reaches the center of the sphere, it is focused and reflected. In the neighborhood of the focal point of a converging wave, temperature gradients increase; therefore, thermal conduction and radiation become the main mechanisms of energy dissipation to be considered when taking into account heat transfer. Maximum densities and temperatures at the center of the sphere and their average values in its regions were calculated. In addition, the time when shock and heat waves cross the sphere center was determined, and their behavior before and after focusing at the sphere center was estimated. It is shown that solutions to such problems can be found much faster and with adequate accuracy when applying simplified models.

Keywords: layered system, shock wave, radiative heat transfer

Received: 26.12.2022 / *Published online*: 01.04.2024

1. Introduction

One of the directions of research of implosion processes (explosion directed not outside, as usual, but inside) on laser installations is mathematical modeling of regimes with acceleration, i.e., such regimes that admit the existence of unbounded solutions for a finite time interval. Previously, such problems were considered in work [1] to study the behavior of extreme solutions. These include shockless compression in gas dynamics, thermal explosion problems, shock wave cumulation processes, and others [2, 3]. Modeling of the joint with gasodynamics of the heat transport system by radiation can significantly affect solutions of such problems, in particular, to make unbounded solutions limited, but with delta-like behavior of the basic quantities. Therefore, there is an interest in processes close to the regimes with consolidation, but with simultaneous consideration of radiative transfer and gas dynamics.

The problem of a descending spherical shock wave was first solved by the German scientist G. Huderlei in 1942 [4] and, independently of him, by L. D. Landau and K. P. Stanyukovich in 1944 [5]. In general form, a description of the motion of a spherical shock wave can be found in the books [6, 7]. When the shock wave arrives at the center, it is focused at the center and reflected from it. Temperature gradients increase near the focus point of the convergent wave, so that heat conduction and radiation become the main mechanisms of energy dissipation when heat transfer is taken into account. The problem of a converging spherical shock wave with accounting for radiative heat conduction was solved by E.I. Zababakhin and V.A. Simonenko [8], who showed that heat conduction modifies the nature of the process: instead of finite density and infinite temperature, infinite density and finite temperature appear. Due to heat conduction, a zone called the thermal precursor appears in front of the shock front, in which the gas not only heats up but also begins to move and thicken.

The cumulative effect can be obtained in other ways. It was demonstrated in [9] that density and pressure can increase in a layered system of alternating light and heavy planar layers. It is much more difficult to describe the motion of a shock wave in a layer system than in a homogeneous medium, so such systems are modeled mainly by numerical methods. Accordingly, the degree of cumulation is much higher in spherical geometries than in planar geometries because the shock wave is amplified by the summation of two factors: sphericity and layering. In [10], a test problem of compression of a simple spherical system consisting of two substances is proposed, taking into account radiation transport in different approximations. It is shown that in compression by shock waves the peculiarity of the problem is a sharp increase in the density of the substance in the center of the sphere. The maximum density is reached after the third shock wave has passed. Such regimes, when the average densities of substances become greater by a factor of tens, can apparently also be attributed to problems with acceleration. Before the steady-state regime is reached, the

main gas-dynamic quantities in this problem (temperature, density, pressure, and velocities of substance boundaries) are oscillating functions. The oscillations of all quantities arising under the influence of strong shock waves are very sharp and require precision methods for their qualitative reproduction. The advantage of the proposed problem is that all radiant transfer approximations analyzed in its formulation give close results for the basic thermodynamic quantities, and when the steady-state regime is reached, their exact values are the same for all approximations.

Earlier in [11], for testing multidimensional programs describing radiative gas dynamics processes, we considered problems of compression by shock waves of a spherical layered system consisting of several substances, with joint consideration of radiative heat conduction and gas dynamics. The peculiarity of these problems is — the attainment of maximum density after the passage of the second or third shock wave. In [12], one of these problems was modeled in the kinetic formulation with minor modifications. The behavior of finite-difference schemes for the kinetic transport equation was studied. In the present work, six simplified models of radiative transfer are additionally applied to solve the same problem.

2. System of equations of high-temperature gas dynamics

In mathematical modeling, the system of equations of high-temperature gas dynamics [13] is split by physical processes and at each time step is solved in two steps. At the first stage, the gas dynamics equations — laws of conservation of mass, momentum, and energy of gas are calculated (gas dynamic motion is represented in the Eulerian-Lagrangian coordinate system according to the method [14]):

$$\frac{d\rho}{dt}+\rho\nabla\cdot\mathbf{u}=0,$$

$$\rho\frac{d\mathbf{u}}{dt}+\nabla P=0,$$

$$\rho\frac{dE}{dt}+P\nabla\cdot\mathbf{u}=0.$$

Here: t — time; ρ — the density of matter; $\mathbf{u}$ — the gas dynamic velocity vector; ∇ — the vector differential operator; $P=p+p_r$ — the total pressure, with $p\,(\rho,T)$ — its gas dynamic component and $p_r=\sigma T_r^4/3$ — the radiation pressure; $T\,(\mathbf{r},t)$ — the temperature of matter; $\mathbf{r}$ — the radius-vector of an arbitrary point in the system; $T_r=\sqrt[4]{\int Id\mathbf{\Omega}/(A\sigma)}$ — radiation temperature; $I(\mathbf{r},\mathbf{\Omega},t)$ — radiation intensity; $\mathbf{\Omega}$ — the unit vector of the photon flight direction; σ — the Stefan-Boltzmann constant; c — the velocity of light; $E(\rho,T)$ — the specific internal energy. In the second step, the change in internal energy due to radiant heat transfer is calculated in various approximations on the basis of the kinetic model. The kinetic model has the form [12]:

$$\frac{\rho}{c}\frac{d}{dt}\left(\frac{I}{\rho}\right)+\mathbf{\Omega}\cdot\nabla I+(\alpha_c+\alpha_s)I=\frac{\alpha_c}{4\pi}B+\frac{\alpha_s}{4\pi}U,$$

$$\rho\frac{dE}{dt}=\alpha_c(U-B).$$

Here: $\alpha_c\,(\rho,T)$ — absorption coefficient,[cm^{-1}]; $\alpha_s\,(\rho,T)$ — scattering coefficient,[cm^{-1}]; $B\,(T)=A\sigma T^4$; $U(\mathbf{r},t)=\int Id\mathbf{\Omega}$ — radiation energy density multiplied by the speed of light c.

Let us supplement the system of equations of heat transfer by radiation with initial and boundary conditions:

$$I(\mathbf{r},\mathbf{\Omega},t=0)=I^0(\mathbf{r},\mathbf{\Omega}),\quad I\left(\mathbf{r}\in\bar{\Gamma},\mathbf{n}\cdot\mathbf{\Omega}<0,t\right)=I^-\left(\mathbf{r}\in\bar{\Gamma},\mathbf{\Omega},t\right),\quad T(\mathbf{r},t=0)=T^0(\mathbf{r}),$$

where $\mathbf{n}$ — the external normal to the boundary $\bar{\Gamma}$ of the computational domain Γ.

Let us denote by $\mathbf{S}\,(\mathbf{r},t)=\int\mathbf{\Omega}Id\mathbf{\Omega}$ the radiation energy flux vector. Integrating the transport equation by $\mathbf{\Omega}$ with weights $1,\mathbf{\Omega}$, we obtain a system of equations:

$$\frac{\rho}{c}\frac{d}{dt}\left(\frac{U}{\rho}\right)+\nabla\cdot\mathbf{S}+\alpha_cU=\alpha_cB,$$

$$\frac{\rho\beta}{c}\frac{d}{dt}\left(\frac{\mathbf{S}}{\rho}\right)+\nabla(\mathbf{D}U)+(\alpha_c+\alpha_s)\mathbf{S}=0,$$

where $\mathbf{D}=\{D_{ij}\}$ — symmetric tensor of quasi-diffusion coefficients and β — a parameter that determines the kind of approximation with which radiant heat transfer is considered:

$$\beta=1,\ D_{ij}=U^{-1}\int \Omega_i\Omega_j I d\mathbf{\Omega} \text{ — hyperbolic quasidiffusion (QD)[15],}$$

$$\beta=0,\ D_{ij}=U^{-1}\int \Omega_i\Omega_j I d\mathbf{\Omega} \text{ — parabolic quasidiffusion (PQD) [16],}$$

$$\beta=1,\ D_{ij}=\delta_{ij}/3 \text{ — P1 [17],}$$

$$\beta=1/3,\ D_{ij}=\delta_{ij}/3 \text{ — P1/3 [18],}$$

$$\beta=0,\ D_{ij}=\delta_{ij}/3 \text{ — diffusion (DF) [19],}$$

δ_{ij} — the Kronecker symbol ($i,j=1\div n$, n — dimensionality of space $\mathbb{R}^{\mathrm{n}}$).

The corresponding initial and boundary conditions are of the form:

$$U(\mathbf{r},t=0)=U^0(\mathbf{r}),\quad \mathbf{S}(\mathbf{r},t=0)=\mathbf{S}^0(\mathbf{r}),\quad T(\mathbf{r},t=0)=T^0(\mathbf{r}),\quad \bar{\alpha}U-\bar{\beta}(\mathbf{n}\cdot\mathbf{S})=\bar{\gamma}.$$

Here $\bar{\alpha}$, $\bar{\beta}$, $\bar{\gamma}$ — parameters of the boundary conditions, with $\bar{\alpha}\geqslant 0$, $\bar{\beta}\geqslant 0$, $\bar{\alpha}+\bar{\beta}>0$.

In numerical modeling of the kinetic equation of transport, various assumptions [13] are used to reduce the number of variables, counting time, and the amount of memory occupied by the computer, allowing the problem to be reduced to a simpler one. For example, assuming a linear dependence of the radiation intensity on the direction of particle flight, we find the P1 approximation of the spherical harmonics method. Further, expecting that there is a dependence between the density and the radiation flux in the form of Fick's law, we obtain the diffusion approximation. Assuming that the approximate equality $U=B$ (the condition of local thermodynamic equilibrium) is valid, we arrive at the sixth, simplest approximation of radiative heat conduction (RHC). In optically transparent media, the DF and LTP approximations give overestimated values of the radiative flux, so it is desirable to limit the heat flux to the maximum permissible value when calculating with these approximations. In the problem discussed in the next section, the heat flux values do not exceed the maximum permissible values because of the sufficient optical density of the system.

The P1 model, in contrast to the DF and LTP approximations, keeps the photon propagation velocity finite, which in the general case is less than the speed of light. This is corrected in the P1/3 approximation proposed in [18] by introducing a 1/3 multiplier in front of the time derivative of the flux. By asymptotic analysis, G. Morel showed [20] that the characteristics of the models in the P1/3 and P1 approximations are close.

The results of both the P1 and P1/3 approximations are presented below. The CD approximation accounts for kinetic effects by using coefficients that are fractional linear functionals of the solution, which makes it the closest to the kinetic model. Algorithms for solving the heat transport equation by radiation for models with different approximations are described in [21, 22]. The method for solving the LTP equation is taken from [14].

3. Test Problem Statement

We consider a ball of radius $0\leqslant r\leqslant R_2$ consisting of two physical regions (Table 1). The inner region 1 ($0\leqslant r\leqslant R_1$) is formed by matter of density $\rho_1=0.02$ g/cm^3, the outer region 2 ($R_1\leqslant r\leqslant R_2$) — matter of density $\rho_2=1$ g/cm^3. The equation of state of each of substances is represented as $P=0.54\rho T$ and $E=c_V T$, where $c_V=0.81T$ — constant heat capacity. The ball, as a system, has an initial temperature of $T^0=0.00001$ keV, and an initial velocity of $\mathbf{u}=0$. At the outer boundary of the system, the pressure in conditional units (1 u.e.=10^8 TPa) $P_{R_2}=0.1$ u.e. and the temperature $T_{R_2}=0.1$ keV are given. The problem formulation is described in [11], but here, for simplification, the absorption coefficient is taken to be the same in both regions. The absorption coefficient is calculated by the formula: $\alpha_c=(\rho/5)\left[\left(1+8.65/\left(\rho^{2/3}T^2\right)\right)^{3/2}-1\right]$, the scattering coefficient — by the formula: $\alpha_s=\rho/5$.

In the numerical realization, the computational difference grid is chosen based on the data on the convergence to the exact solution. Before the steady-state regime is reached, all quantities are oscillating functions, and at $t\to\infty$ the solution of the problem reaches constant values:

$$\mathbf{u}=0,\quad P=1\text{ TPa},\quad T=0.1\text{ keV},\quad R_{1,st}=R_1\sqrt[3]{\rho_1^0/\rho_{st}}\approx 0.11\text{ cm},$$

Table 1. System composition

Parameter	Area number	
	12	
Initial density ρ^0, g/cm^3	0.02	1
Initial radii $R_{1,2}$, cm	0.5	0.6
Number of difference grid cells	100×30	400×30

$$R_{2,st} = \sqrt[3]{(1/\rho_{st})[R_1^3\rho_1^0 + (R_2^3 - R_1^3)\rho_2^0]} \approx 0.37 \text{ cm}, \quad \rho_{1,2} = \rho_{st} \approx 1.851 \text{ g/cm}^3.$$

The lower index *st* indicates that the quantity corresponds to the stationary regime.

4. Simulation results

The calculations were performed using a two-dimensional program developed by the authors in the RFNC-VNIITF for axisymmetric cylindrical geometry until the maximum values of density and temperature were reached in the 1st region (0.13μs). Then, as time passes, the density and temperature values change in the form of pulsations with out to the stationary regime.

The convergence constant of iterations on temperature was assumed to be 10^{-5}, the quadrature on the directions of particle flight — ES_{16}. The time step was varied to account for the behavior of the solution, but did not exceed 1 pc.

The maximum values of the main gasdynamic quantities (temperature, pressure, and density) are reached in the center of the sphere. The calculation data, namely, the maximum values of the mean temperature $T_{\max}$ and mean density in the 1st region, the computer counting times ($t_{\rm CP}$), the arrival of thermal ($t_{\rm TW}$) and shock ($t_{\rm SW}$) waves at the center of the sphere and their differences Δin percent from the results of the kinetic model are given in Table 2. The average density and temperature of matter are calculated by formulas $\rho = \sum_i \rho_i V_i / \sum_i V_i$, $T = \sum_i T_i M_i / \sum_i M_i$, where ρ_i and T_i — density and temperature in the center of a cell with index i having volume V_i and mass M_i.

Table 2. Calculation results

Models	$T^1_{\max}$,keV	$\Delta T_{\max}$,%	$\rho^1_{\max}$,g/cm^3	$\Delta\rho_{\max}$,%	t_{rmTW},μs	$\Delta t_{\rm CP}$,%	$t_{\rm SW}$,μs	Δt_{rmSW},%	$t_{\rm CP}$,hour
Kinetic	0.41036	0	89.04680	0	0.67964	0	0.82870	0	24
KD	0.41247	0.52	88.18494	0.97	0.68594	0.93	0.82520	0.42	11
PKD	0.41248	0.52	88.20339	0.95	0.68595	0.93	0.82526	0.42	11
R1	0.41134	0.24	88.68709	0.40	0.68594	0.92	0.82536	0.40	2
R1/3	0.41134	0.24	88.69607	0.39	0.68595	0.93	0.82537	0.40	2
DF	0.41134	0.24	88.70132	0.39	0.68595	0.93	0.82536	0.40	2
LTP	0.40294	1.80	80.57137	9.52	0.66174	2.63	0.82142	0.99	0.5

Table 2 shows that all approximations, except LTP, show sufficiently good agreement (the difference is less than 1%) with the kinetic model for the quantities under consideration. The kinetic model is the most costly in terms of counting time, although it uses parallelization by photon flight direction. The LTP approximation looks the most economical, but it gives the maximum differences from the kinetic model. For different approximations, the steady-state regime is reached in 10 μs faster, compared to the kinetic calculation, approximately from 2 to 50 times, so it is rational to use approximate models.

Since for the results analyzed below, the transport models used, with the exception of LTP, give visually indistinguishable plots, only the LTP and KD approximations are presented in the figures for comparison. The drawing 1 shows the dependences on time of the average density and temperature of substances in the regions. It can be seen that for the entire calculation time, both approximations agree well on average temperatures and average densities. The largest difference is observed during the heating of region 1, where the difference in data of LTP and CD at the moment of time 0.075 μs is 10%. However, by time 0.113 μs, when the mean temperature reaches a maximum, the discrepancy decreases to 1.8%. We also note that there is a discrepancy in the mean densities at the time of maximum compression of the 1st region at 0.117 μs: the difference between the densities found by the LTP and KD approximations is about 9%.

As shown in [11], the system under consideration is optically dense, so in different models the average matter temperatures and average radiation temperatures do not differ in thecurrent of the entire counting time. However, in separate points, in particular, in the center of the sphere, they can be very different, i.e., there is a "breakaway" of temperatures.

The figure 2 demonstrates the "separation" of temperatures at the moments of the arrival of shock waves at the center of the sphere (0.0832 and 0.1125 μs). It follows from the figure that the temperature of matter almost instantaneously — in the time of 0.4 ns, increases at the first peak by a factor of 10 (from $T \approx 0.3$ keV to $T \approx 3.9$ keV)

and exceeds the radiation temperature $T_r \approx 0.65$ keV by a factor of 6. To analyze the behavior of the shock and heat waves, the profiles of the main thermodynamic quantities at different time moments are presented in semilogarithmic scale in the figure 3: at the approach of the heat wave to the contact rupture— 0.025 μs; at the approach of the heat wave to the center of the system— 0.065 μs; at the moment following the time of reflection of the shock wave from the center of the sphere— 0.088 μs. The contact rupture is represented by a vertical dashed line and the distances to the center of the sphere $R=\sqrt{r^2+z^2}$ correspond to it, respectively, cm: 0.1047; 0.2621; 0.4987.

The drawing 3*a* shows the dependences on the distance to the center of the system R of profiles T, P, ρ at time close to the arrival of the heat wave to the contact rupture. It can be seen that four zones can be distinguished: the zone of unperturbed cold matter ($0<R<0.498$ cm, $\rho=0.02$ g/cm^3, $T=10^{-5}$ keV, $P=10^{-7}$ u.e.); the shock precursor zone ($0.498<R<0.506$ cm, $0.02<\rho<1$ g/cm^3, $T\approx10^{-5}$ keV, $P\approx10^{-5}$ u.e.); the shock wave zone ($R\approx0.506$ cm); the shock wave heated after shock wave zone ($0.506<R<0.535$ cm, $\rho\approx4$ g/cm^3, $0.05<T<0.1$ keV, $P\approx0.1$ u.e.). In this case, the thermal and shock wave fronts coincide.

Figure 3*b* contains profiles T, P, ρ at time close to the arrival of the heat wave at the center of the system. Six zones can be distinguished in the graphs: the zone of unperturbed cold matter ($0<R<0.07$ cm, $\rho=0.02$ g/cm^3, $T=10^{-5}$ keV, $P=10^{-7}$ u.e.); the shock wave precursor zone, where the temperature exceeds the boundary value ($0.07<R<0.21$ cm, $\rho=0.02$ g/cm^3, $T\approx0.15$ keV, $P\approx10^{-3}$ u.e.); the shock wave zone ($R\approx0.21$ cm); the rarefaction wave zone at ($R\approx0.3$ cm); the zone between the shock wave and the rarefaction wave ($0.21<R<0.3$ cm); the zone in front of the rarefaction wave ($0.3<R<0.41$ cm). In this case, the heat wave front is ahead of the shock wave front by about 0.14 cm. The temperature rise above the boundary value in the zone between thermal waves ($0.07<R<0.3$ cm) is explained by the transfer of part of the kinetic energy to thermal energy due to the compression of matter.

Figure 3*c* shows the profiles of T, P, ρ after the shock wave is reflected from the center. Three zones are seen: the zone after the passage of the reflected shock wave ($0<R<0.025$ cm); the zone from the reflected heat wave to the reflected shock wave ($0.025<R<0.185$ cm); and the zone before the reflected heat wave ($0.185<R<0.31$ cm). After the shock wave is reflected from the center, the system is fully heated, and the reflected heat wave front is ahead of the reflected shock wave front by about 0.17 cm. Secondary heating and compression waves in the 2nd region of the ball create a nonmonotonic pattern of behavior of the quantities T, P, ρ in the third zone.

5. Conclusions

The paper tests various approximate models of heat transfer by radiation on the problem of compression of a spherical system by shock waves. The results of calculations aimed at finding the maximum values of densities and temperatures both in the center of the sphere and their average values in the regions, as well as at determining the arrival times of shock and heat waves in the center of the system, are presented. The passage of shock and heat waves through the contact rupture and their behavior before and after focusing in the center of the system are investigated. It is shown that problems of this type can be solved much faster using simplified models.

The results allow us to draw the following conclusions:

1) The substance-averaged temperatures and densities coincide in all models to within 1%, with the exception of the

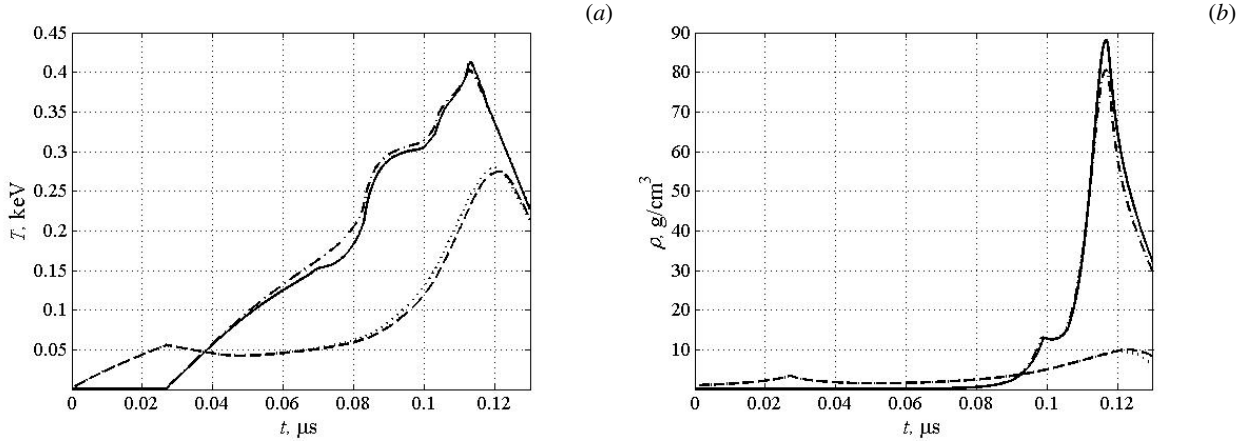

Fig. 1. Time-dependent mean values of temperature (*a*) and density (*b*) for two approximations of radiative heat transfer: Region 1 – LTP (dashed line), KD (solid); Region 2 – LTP (dotted line), KD (dashed)

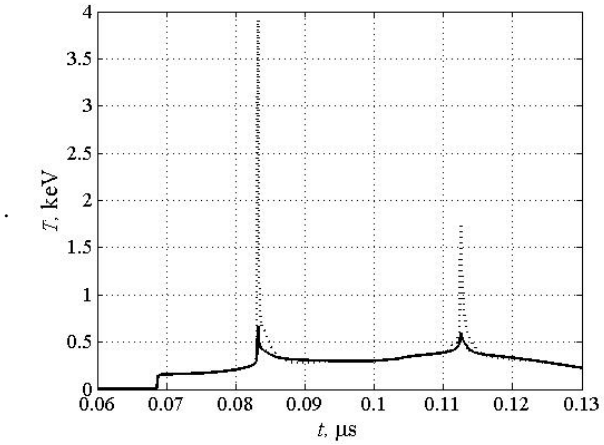

Fig. 2. Temperatures at the center of the sphere for the CD approximation: matter temperature (dotted line), radiation temperature (solid line)

LTP. In the LTP approximation at the moment of maximum compression, the difference from the kinetic model in the mean density in the 1st region reaches 9.5%, and the maximum mean temperature — 1.8%.

2) The temperature "breakaway" effect is observed only at the points of maximum compression in all models except LTP, where it is not possible. The temperature of matter at the points of maximum compression can exceed the radiation temperature by a factor of more than 6.
3) The range of the arrival time at the center of the system of a heat wave according to the considered models, except LTP, is rather small, about 0.6 ns, the arrival time of a shock wave about — 0.4 ns. In the LTP approximation, the arrival time at the center, in comparison with the kinetic model, is smaller by about 2 ns for the thermal wave and

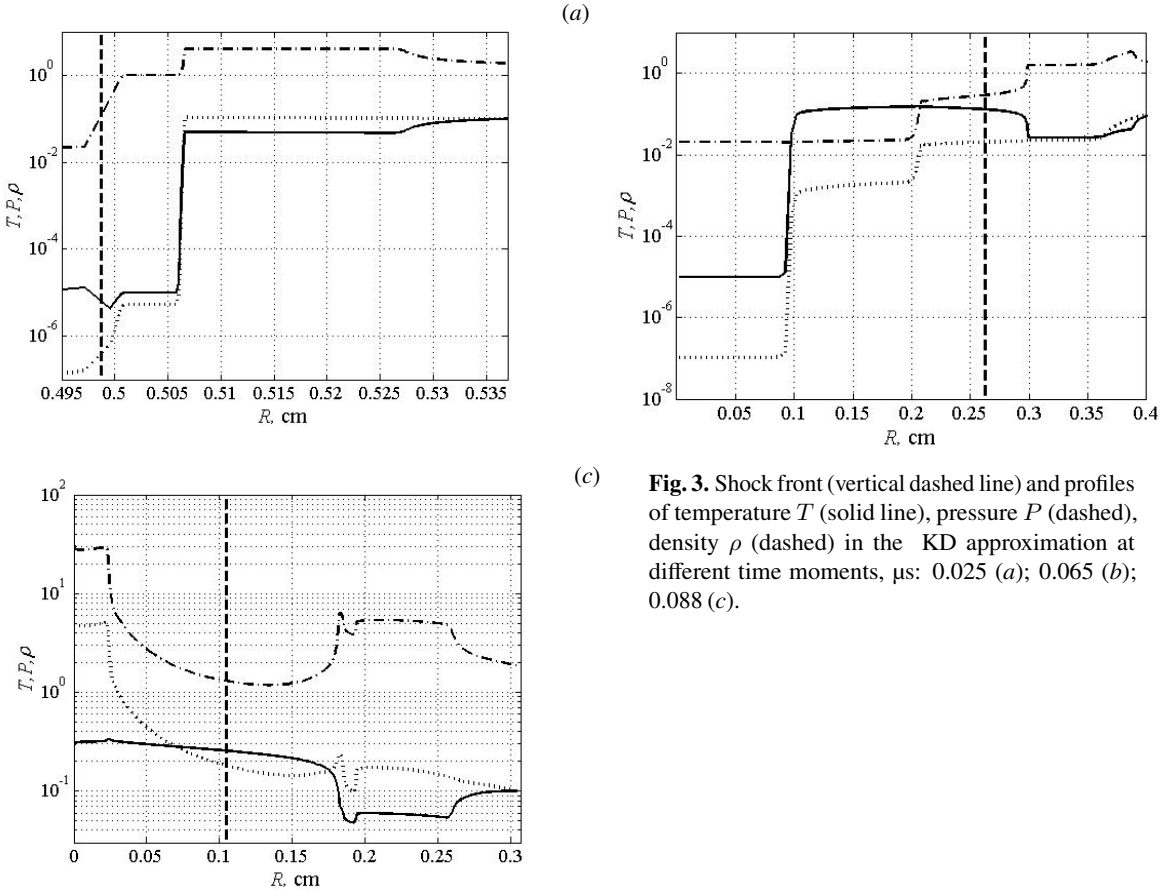

Fig. 3. Shock front (vertical dashed line) and profiles of temperature T (solid line), pressure P (dashed), density ρ (dashed) in the KD approximation at different time moments, μs: 0.025 (*a*); 0.065 (*b*); 0.088 (*c*).

by about 0.7 ns for the shock wave.

4) By the time the shock wave approaches the contact rupture and the center of the system, a thermal precursor zone can be identified. This is the difference between the described test formulation and classical formulations of shock-wave problems such as penetration, shock-wave loading, breakaway phenomena, and others, where thermal conductivity does not play a significant role.
5) Although in spherical layers the degree of cumulation may be much higher than in planar layers, the thermal radiation accounted for in this problem gives a finite density and temperature at the moment of focusing, which is confirmed by calculations in models of different degrees of approximation.
6) Before the moment of focusing, a heating zone appears in the center of the system before the shock wave in the 1st region due to radiation, in which the matter reaches a temperature higher than the boundary temperature. At the moment of focusing in the center of the system, the temperature of the matter increases by a factor of more than 10.
7) In the problem under discussion, the counting time in KD and PKD approximations is about two times less than the counting time of the kinetic model (taking into account parallelization by directions of photon flight), in DF, P1, and P1/3 approximations — 12 times less, in LTP approximation — 48 times less.
8) The coincidence of the results of the kinetic model and in the DF approximation shows a reasonably good accuracy and monotonicity of the TVDR (Total Variation Diminishing Reconstruction) [21] kinetic scheme of higher approximation order, since the DF approximation uses a second-order approximation scheme in space [22]. The classical monotonic first-order approximation scheme for the kinetic model gives a difference from the TVDR scheme in the time of arrival of the heat wave in the center of the system of about 26% [12].

The test problem and the results obtained by the authors can be used to study the processes of compression of substances by shock waves and to test the methods of high-temperature gas dynamics that take into account heat transfer by radiation in different approximations.

References

1. *Samarskii A.A.*, *Galaktionov V.A.*, *Kurdyumov S.P.*, *Mikhailov A.P.* Blow-Up in Quasilinear Parabolic Equations. De Gruyter, 1995. 535 p.
2. *Danilenko V.V.* Explosion: physics, engineering, technology. Energoatomizdat, 2010. 784 p. (in Russian).
3. *Sysoev N.N.*, *Selivanov V.V.*, *Khakhalin A.V.* The Physics of Burning and Explosion. Moscow University Press, 2018. 237 p. (in Russian).
4. *Guderley K.G.* Strake kugelige und zylindrische Verdichtutungsstosse in der Nane des Kugelmittelpunktes bzw. der Zylinderachse. Luftfahrtforschung. 1942. Vol. 19. P. 302–312.
5. 57 - ON A STUDY OF THE DETONATION OF CONDENSED EXPLOSIVES. 1965. DOI: `https://doi.org/10.1016/B978-0-08-010586-4.50062-6`.
6. *Stanyukovich K.P.* Unsteady Motion of Continuous Media. Elsevier, 2016. 960 p.
7. *Zeldovich Y.*, *Raizer Y.P.* Physics of Shock Waves and High-Temperature Hydrodynamic Phenomena. Academic Press, 1967. 478 p.
8. *Zababakhin E.I.*, *Simonenko V.A.* A convergent shock wave in a heat-conducting gas. JAMM. 1965. Vol. 29, no. 2. P. 334–336. (in Russian).
9. *Zababakhin E.I.*, *Zababakhin I.E.* Unlimited Cumulation Phenomena. Moscow: Nauka Publ., 1990. 175 p.
10. *SHestakov A.A.* Ob odnoj testovoj zadache szhatiya sloistoj sistemy s uchetom perenosa izlucheniya v razlichnyh priblizheniyah. Voprosy atomnoj nauki i tekhniki. Seriya: Matematicheskoe modelirovanie fizicheskih processov. 2017. Вып. 4. С. 25–31.
11. *Shestakov A.A.* Test problems on shock compression of layered spherical systems. Mathematical Models and Computer Simulations. 2021. Vol. 13, no. 12. P. 29–42. (in Russian) DOI: `10.1134/S2070048221040207`.
12. *Grabovenskaya S.A.*, *Zaviyalov V.V.*, *Shestakov A.A.* Calculations of Compression of a Spherical Layered System by Shock Waves Taking into Account the Transfer of Thermal Radiation in the Kinetic Model. Fluid Dynamics. 2023. Vol. 58, no. 4. P. 511–519. DOI: `10.1134/S0015462823600475`.
13. *Chetverushkin B.N.* Mathematical modelling of dynamical problems of radiating gas. Moscow: Nauka Publ., 1985. 304 p. (in Russian).
14. *Bicyapin A.Y.*, *Gpibov B.M.*, *Zubov A.D.*, *Heuvazhaev B.E.*, *Pepvinenko H.B.*, *Fpolov B.D.* Komplekc TIGP dlya paccheta dvumepnyx zadach matematicheckoj fiziki. Voprosy atomnoj nauki i tekhniki. Seriya: Matematicheskoe modelirovanie fizicheskih processov. 1984. Issue 3. P. 34–41.

15. *Goldin V.* A quasi-diffusion method of solving the kinetic equation. USSR Computational Mathematics and Mathematical Physics. 1964. Vol. 4, no. 6. P. 1078–1087. DOI: 10.1016/0041-5553(64)90085-0.

16. *Dolgoleva G.V.* Metodika rascheta dvizheniya dvuhtemperaturnogo izluchayushchego gaza (SND). Voprosy atomnoj nauki i tekhniki. Seriya: Matematicheskoe modelirovanie fizicheskih processov. 1983. Vol. 13, issue 2. P. 29–33.

17. *Jeans J.H.* The equations of radiative transfer of energy. Monthly Notices of the Royal Astronomical Society. 1917. Vol. 78, issue 1. P. 28–36.

18. *Olson G.L.*, *Auer L.H.*, *Hall M.L.* Diffusion, P1, and other approximate forms of radiation transport. Journal of Quantitative Spectroscopy and Radiative Transfer. 2000. Vol. 64. P. 619–634. DOI: 10.1016/S0022-4073(99)00150-8.

19. *Bell G.I.*, *Glasstone S.* Nuclear Reactor Theory. Van Nostrand Reinhold Company, 1970. 619 p.

20. *Morel J.* Diffusion-limit asymptotics of the transport equation, the P1/3 equations, and two flux-limited diffusion theories. Journal of Quantitative Spectroscopy and Radiative Transfer. 2000. Vol. 65. P. 769–778. DOI: 10.1016/S0022-4073(99)00148-X.

21. *Gadzhiev A.D.*, *Zavyalov V.V.*, *Shestakov A.A.* Primenenie TVD-podhoda k DS$_N$-metodu resheniya uravneniya perenosa teplovogo izlucheniya v osesimmetrichnoj RZ-geometrii. Voprosy atomnoj nauki i tehniki. Seriya: Matematicheskoe modelirovanie fizicheskih processov. 2010. № 2. C. 30–39.

22. *Grabovenskaya S.A.*, *Zavyalov V.V.*, *Shestakov A.A.* Konechno-obemnaya shema GROM dlya resheniya perenosa izlucheniya kvazidiffuzionnym metodom. Voprosy atomnoj nauki i tehniki. Seriya: Matematicheskoe modelirovanie fizicheskih processov. 2014. № 3. C. 47–58.

Authors' Details:

Svetlana Aleksandrovna Grabovenskaya; e-mail: s.a.grabovenskaya@vniitf.ru; ORCID: 0009-0008-8613-0776

Zavyalov Vyacheslav Viktorovich (corr.); e-mail: v.v.zaviyalov@vniitf.ru; ORCID: 0009-0006-8548-5984

Shestakov Alexander Alexandrovich; e-mail: aashestakov@vniitf.ru; ORCID: 0009-0009-5569-0946